Assessment of volcanic hazards of El Misti and in the city of Arequipa, Peru, based on GIS and simulations, with emphasis on lahars

Gwenaël Delaite, Clermont-Ferrand, Jean-Claude Thouret, Clermont-Ferrand, Michaël Sheridan, Buffalo, NY, Philippe Labazuy, Clermont-Ferrand, Adam Stinton, Buffalo, NY, Thierry Souriot, Clermont-Ferrand, and Cees Van Westen, Enschede

with 10 figures and 1 table

Summary.   Our study aims to assess the volcanic and hydrological hazards and risks on El Misti volcano and in the city of Arequipa in southern Peru, which are exposed to the effects of tephra fall, pyroclastic flows, debris avalanches, lahars, and floods. Arequipa, Peru's second city, is home to approximately 850,000 people who live in the shadow of El Misti volcano whose summit is located approximately 3.5 km vertically and 17 km horizontally to the NE of the city centre. Since 1990, Arequipa has undergone unprecedented and largely uncontrolled urban expansion, with new settlements being constructed on the volcano's SW and S flanks and along radial valleys within 9-11 km of the summit. The purpose of this work is to assess hazards of tephras falls, pyroclastic flows, and lahars based on geologic record, mapping, statistical analysis, and GIS techniques. Three hazard zone maps portray a probable small-scale vulcanian eruption scenario, a mid-range sub-Plinian eruption scenario and a large-scale Plinian eruption scenario. Our emphasis here is on lahars and on simulating debris flows and hyperconcentrated flows by using the semi-empirical code LAHARZ. Output maps show that all simulated lahars with anticipated volumes in the range of 1.5 to 11 million m^3, can be conveyed across the city of Arequipa through the Río Chili valley and three tributary drainages termed Quebradas San Lazaro, Huarangal, and Agua Salada.

Résumé: *Evaluation des aléas et des risques, notamment ceux des lahars, autour du volcan actif El Misti et dans la ville d'Arequipa (Pérou), fondée sur les SIG et les codes de simulation.* Notre étude vise à évaluer les aléas et les risques volcaniques et hydrologiques dans la région du volcan El Misti et de la ville d'Arequipa au sud du Pérou, qui est exposée aux effets des retombées, des écoulements pyroclastiques, des avalanches de débris, des lahars et des inondations. La ville d'Arequipa, seconde en importance après Lima au Pérou, abrite presque un million d'habitants à proximité du volcan El Misti situé à 3500 m au-dessus et à 17 km au NE du centre ville. Depuis les années 1990, la ville a connu une expansion rapide et incontrôlée dans l'oasis et en direction du volcan, qui s'est traduite par de nouveaux quartiers construits sur les flancs SW et W et dans les vallées radiales du Misti en direction de la ville. Le but de ce travail est d'évaluer quantitativement les aléas et les risques liés aux retombées, aux coulées pyroclastiques et surtout aux lahars : les scénarios éruptifs, les bases de données incorporées dans le SIG ILWIS et les simulations réalisées avec le code LAHARZ ont été combinés. Les résultats exprimés sous la forme d'un double zonage montrent que presque tous les lahars, simulés selon quatre catégories de volume de 1.5 à 11 million m^3, traversent toute la ville d'Arequipa, comme le suggèrent les dépôts des terrasses fluviales datés de l'Holocène supérieur et de la période historique dans la zone urbanisée.

1   Introduction

Large cities worldwide gather tens of million of people who now live under the shadow of active volcanoes within a distance of tens of kilometres, such as Napoli in southern Italy (CHESTER 2000). Arequipa in southern Peru is a spectacular case study because almost one million people

live within 17 km distance from the summit of the active El Misti volcano. In the recent past, cities like Armero (Colombia) in 1985 have been laid waste in a matter of minutes due to lahars. Thus, objective delineation of hazard zones, assessment of hazardous volcanic phenomena, and tools available for timely emergency planning are a prerequisite. In this paper we present a study of volcanic hazards that the active El Misti composite cone poses to the city of Arequipa, second to Lima in Peru in terms of population at risk and infrastructures at stake.

Our study aims to assess hazards and risks around El Misti volcano and in the city of Arequipa, whose inhabitants are exposed to the effects of tephra falls, pyroclastic flows, debris avalanches, lahars, and floods. Our assessment is based on geomorphological and geological field and laboratory surveys (THOURET et al. 1995, 1999a, 2001, MACEDO 1994, NAVARRO 1998, SUNI 1999). The eruptive history and behavior of El Misti has provided a basis for statistically analyzing the eruption frequency and for embedding geographical and socio-economical data in the Geographical Information System ILWIS (DELAITE 2003). Aiming to emphasize hazards and to delineate lahar-prone areas, we have used the semi-empirical computer code LAHARZ (SCHILLING 1998, IVERSON et al. 1998) to simulate lahars of four volume categories that would flow from El Misti through the drainage system and across the city.

2   Methods for assessing volcanic hazards and risks

2.1 Background and purpose of the work

A blend of traditional and modern methods for assessing hazards has been carried out on active volcanoes (BLONG 1984, 2000): field surveys; geological and geomorphological mapping using a GIS; statistical analysis of event magnitude and frequency; numerical and experimental modelling in laboratory aiming at reproducing some flow processes; geotechnical studies to determine the impact of tephra fall on housing, etc. Here we concentrate on methods which link fundamental to applied research by deriving data from the geological data base; we emphasize GIS integration techniques and the semi-empirical computer code LAHARZ for simulating flows and delineating hazard zones prone to lahars and floods. In addition, the GIS ILWIS is a tool used for integrating output maps of simulated lahar paths with three eruption scenarios as well as for contributing to the management of a future eruption crisis.

2.2 Research flow chart

Firstly, a DEM was calculated based on digitised topographic maps, on Radar interferograms, as well as on stereo-photogrammetry using pairs of aerial photographs (1:5,000 scale) in selected city areas. The overall DEM resolution is 30 m but as precise as 8 m in two valley channels, which cross the city of Arequipa. Secondly, three hazard-zone maps are derived from eruption scenarios, which are based on the detailed eruptive history of El Misti over the past 50 ka (THOURET et al. 2001). Thirdly, GIS encompasses a geo-referenced data base, which combines information layers depicting housing at a block scale, infrastructure, and population density, as well as vulnerability maps. From the geological map, we have drawn a geotechnical map, which portrays a set of materials ranked according to their ability to be remobilised by lahars. Fourthly, the LAHARZ code

(SCHILLING 1998) was run on topographic DEMs for simulating lahar and delineating lahar-prone areas. Input are four ranges of lahar volumes and the H/L energy line computed on the El Misti cone. Outputs of simulations are incorporated in the GIS ILWIS geo-reference database along the four river valleys. Fifthly, these maps are combined in risk maps (using a statistical analysis), which are validated by field surveys carried out on lahar and flood deposits. Such deposits have been measured and dated along profiles across four drainages: Río Chili and its tributaries Quebradas (Qda.) San Lazaro, Huarangal, and Agua Salada (Quebrada, Qda= deep and narrow stream valley, usually dry from April to November).

3 Arequipa, Peru's second city, and the active El Misti volcano

Arequipa, where 850,000 lived in 1995 (probably 1,000,000 in 2005), lies 17 km SW and 3.5 km below the El Misti's active summit crater (Fig. 1). People used to live in the oasis about 15–20 km away from the volcano. Nowadays, suburbs are located 9–11 km away from the active crater while the constructed city area has increased by 600% over the period 1940 to 1997 (Fig. 2). Hazards posed to Arequipa by the future El Misti activity are inferred from our knowledge of the geologic evolution and eruptive behaviour of the volcano.
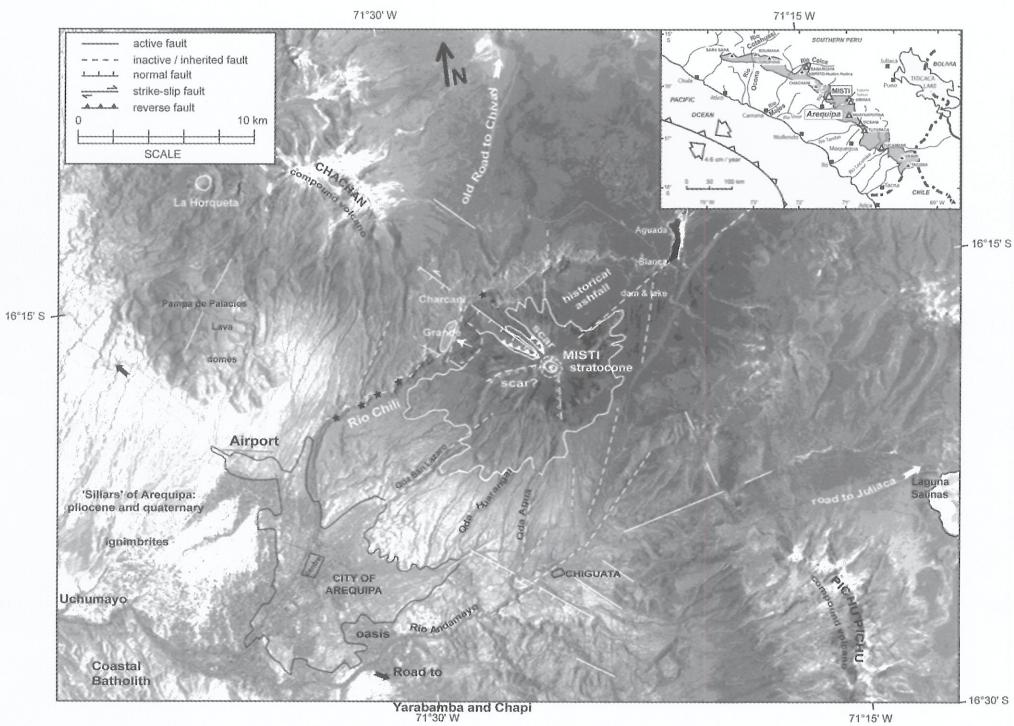

Fig. 1. Landsat extract showing the geomorphological setting of the Arequipa depression, El Misti volcano, and neighbouring volcanoes. Inset: El Misti volcano and Arequipa, and the Pleistocene-Holocene volcanic range in the Central Andean Volcanic Zone in southern Peru.
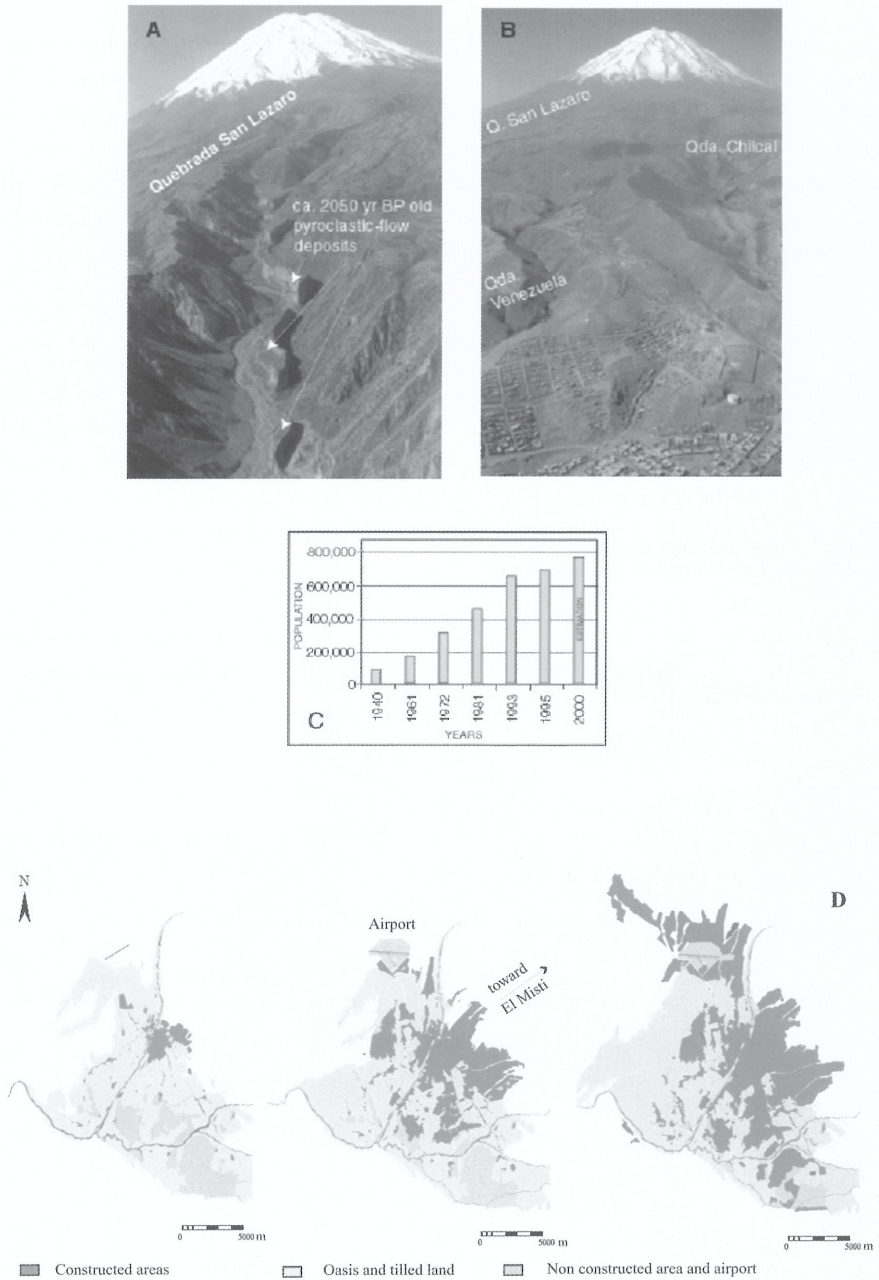
Fig. 2. A. Photograph showing the ca. 2090 yr BP-old pyroclastic-flow deposits in the *Quebrada* San Lazaro located 9 km of the vent and 2 km of the present boundary of the city. B. Photograph showing how the city suburbs have recently spread on the S and SW flanks of El Misti within 11 km of the summit. C. Population growth in Arequipa since 1940 (INEI-ORSTOM 1998). D. Growth of the city of Arequipa in the oasis from 1944 to 1997.

3.1   Summary of the evolution of El Misti composite cone

The evolution of the composite El Misti edifice over the past ca. 833 ka can be divided in four parts (THOURET et al. 2001; Figs. 3 and 4): (1) El Misti 1 stratovolcano, 833 – 112 ka, has been largely built up of voluminous lava flows with some pyroclastic debris. Pleistocene lava flows of El Misti 1 have flowed as far as 11 km towards the depression of Arequipa. (2) El Misti 1 and 2 stratocones, overlapping El Misti 1, are less than 112 ka. (3) Non-welded dacitic ignimbrites, with a bulk volume of 4–6.5 km^3, probably reflect large explosive eruptions on El Misti 3 that have led to the formation of large craters, or an incremental caldera, between 50,000 and 40,000 yr BP. (4) El Misti 4 summit cinder cone was built <11 ka in the summit large crater or caldera, which was formed around 13,700 and 11,300 yr BP ago.

Since the building of El Misti 2, repeated episodes of dome growth and destruction have triggered dome-collapse avalanches and block-and-ash flows, as well as pyroclastic surges. The dome-building episodes alternated with sub-Plinian eruptions whose high-column collapses generated pyroclastic flows. The last sub-Plinian explosive episode ca. 2090 ± 80 yr BP (cal. 400 BC – 340 AD) produced a pumice fall and flows 0.7 to 1 km^3 in volume. The most recent eruption occurred in AD 1440–1470, while phreatic events were reported in 1677, 1784, and 1787 (ZAMÁCOLA & JAÚREGUI 1804, BARRIGA 1951, HANTKE & PARODI 1966; CHÁVEZ CHÁVEZ 1992; SIMKIN & SIEBERT 1994). The small-sized AD 1440-1470 events dispersed about 6 x 10^6 m^3 of ash fall to the SW and mostly to the North (black area on Landsat satellite scene: Fig. 1). In most recent times, persistent, high-temperature fumarolic activity is observed on the plug inside the youngest nested crater and on the summit east flank.

3.2   Assessment of volcanic hazards of El Misti

Based on composite stratigraphical sections and on >30 dated erupted deposits (Fig. 4: THOURET et al. 2001), the pattern of El Misti's eruptive behavior has significantly evolved towards explosive activity and can be grouped into one of four types:

1) Ignimbrite-forming eruptions produced ash-and-pumice-flow deposits several km^3 in bulk volume on a 10,000 to 20,000 years average interval;

2) Several episodes of dome growth and destruction repeatedly generated dome-collapse avalanches and block-and-ash flows during the past 50 ka;

3) Sub-Plinian eruptions with pumice-fall and flow deposits less than 1 km^3 in volume occurred every 2000 to 4000 years on average;

4) Vulcanian and phreatomagmatic eruptions delivered small volume scoria-fall and ash-and-scoria-flow deposits every 500 to 1500 years on average.

El Misti is a dangerous volcano because its explosive behavior has produced a wide range of deadly and destructive deposits over the past 50 ka: (1) ash fallout of vulcanian eruptions, (2) block-and-ash flows linked to pelean domes, (3) Plinian pumice fallout and pyroclastic flows produced by sub-Plinian and Plinian eruptions, (4) Ignimbrites related to caldera-forming eruptions. The composition of the erupted lavas ranges between mafic andesites 52–57%wt. SiO$_2$ and rhyolites > 69%wt. SiO$_2$. Over the past 2000 years, the explosive activity of El Misti, which has been in turn vulcanian, phreatomagmatic, and sub-Plinian, has produced magma mingling as shown in heterogeneous textures and enclaves of dacitic and mafic andesite in the ca. 2090 yr BP-old pumices.
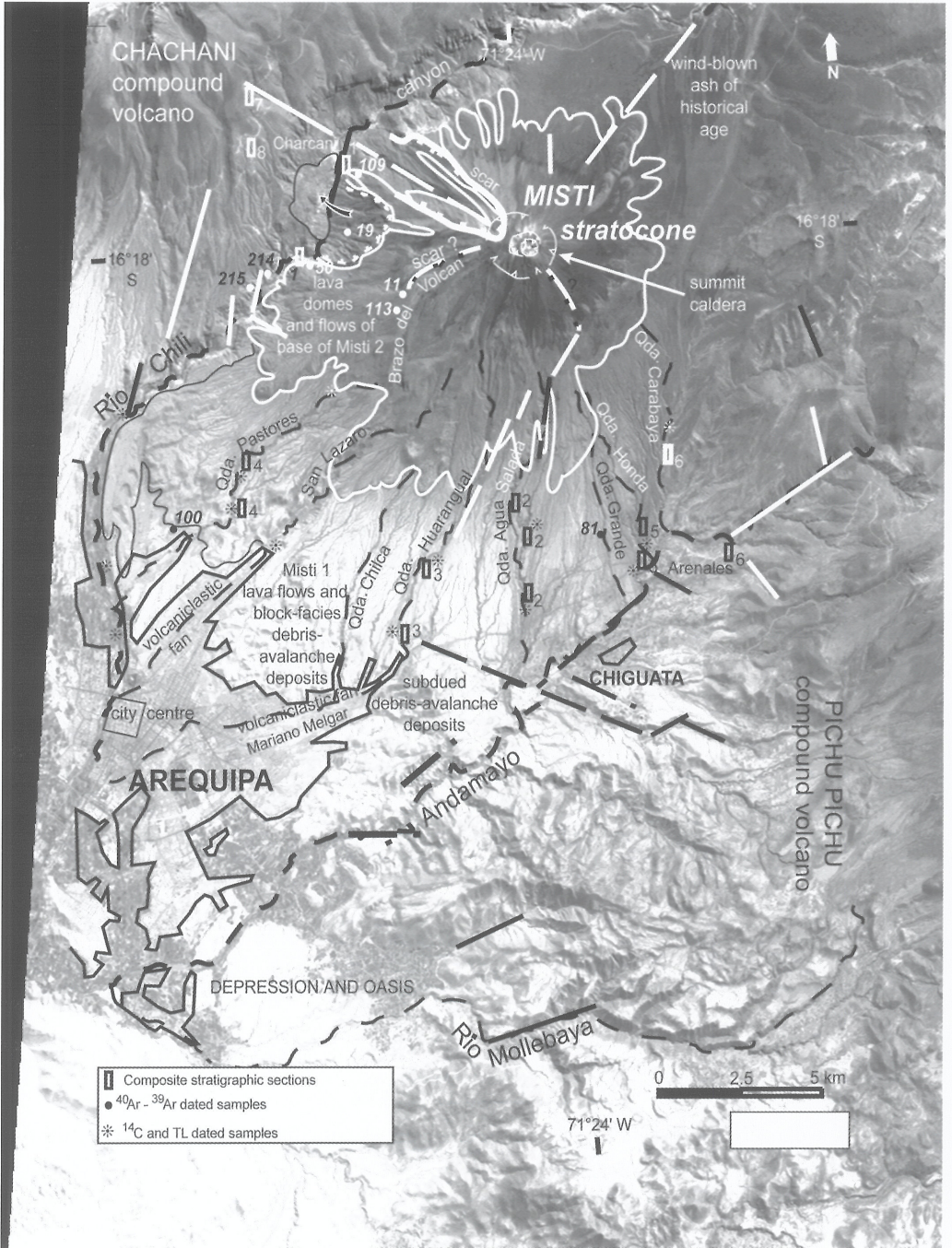
Fig. 3. Geological sketch of El Misti volcano and surrounding areas based on a satellite SPOT scene, on field survey, and on Ar[40]-Ar[39] and ^{14}C age dates (after THOURET et al. 1999a, 2001).
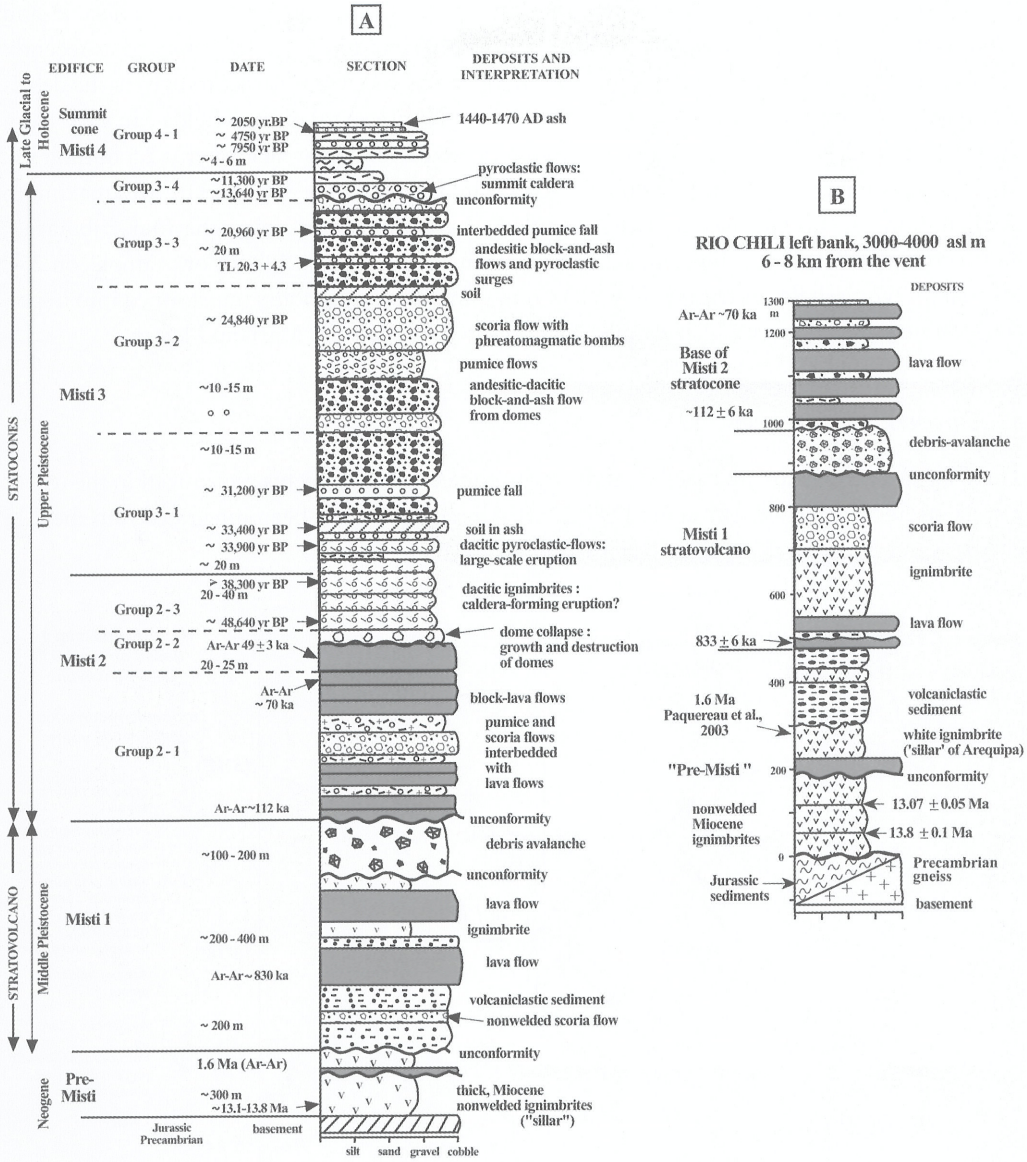
Fig. 4. Composite stratigraphical sections showing seven groups of pyroclastic deposits that form El Misti 1 to 4 composite volcano.

In addition, eruption and/or rainfall-triggered lahars have occurred in the Holocene and
swept down the Río Chili valley and tributaries about 1035 yr and 520 yr BP ago, and as recently
as in the 1600's. Some of these flows were likely triggered by meltwater owing to pyroclastic debris
that have flown onto the summit snow and ice field. As present-day snowfields can vary from
1 to 7 km^2 from January to August, the maximum expected volume of meltwater is 2.5 million m^3.
The overall volume of the channeled debris flows is in the range of 4–5 million m^3 to a maximum
of 11 million m^3. Hyperconcentrated streamflows have also swept down the four tributaries,
which cross the city of Arequipa, on a 2 to 10 years interval (NAGATA 1999). For example, on 25th
February, 1997, flash floods triggered by a 33.4 mm rainfall during 3 hours transformed into hyper-
concentrated streamflows, which claimed 3 victims in the Quebrada Mariano Melgar.

3.3 *Three eruption scenarios*

Three hazard-zone maps are based on three magnitude/frequency events recognized in the recent
history of El Misti (THOURET et al., 1999, 2001). All scenarios have been integrated into the GIS
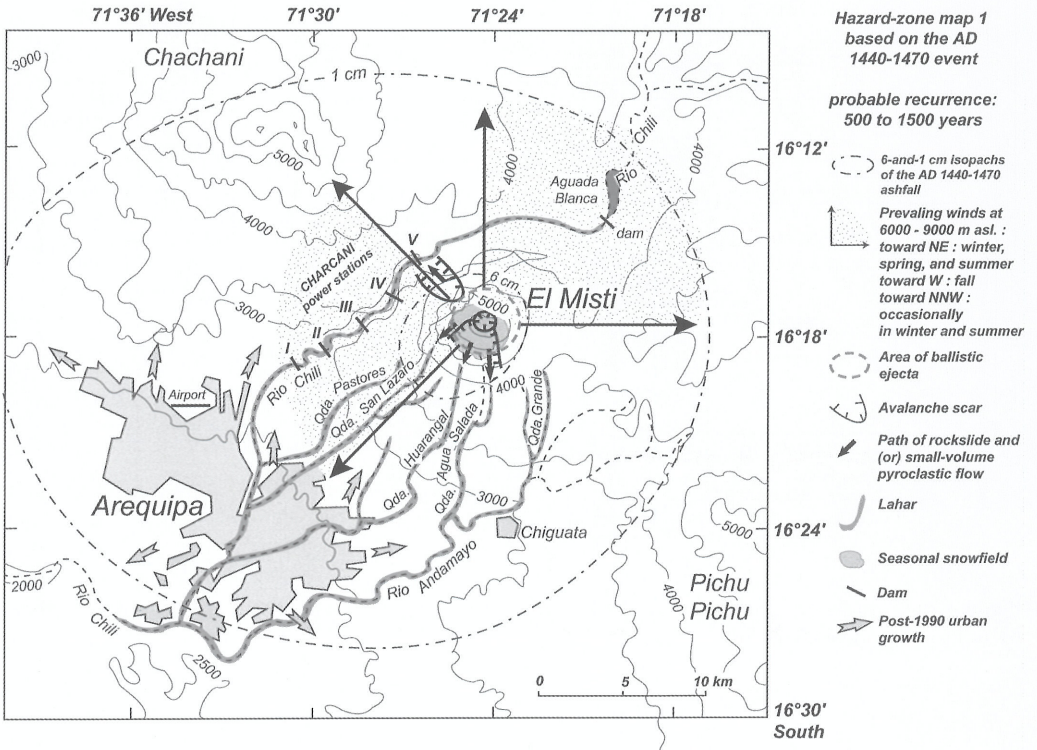database and the outputs are three hazard-zone maps (Figs. 5, 6 and 7).

Fig. 5. Hazard-zone map of El Misti volcano portraying the effects of the most probable eruption scenario
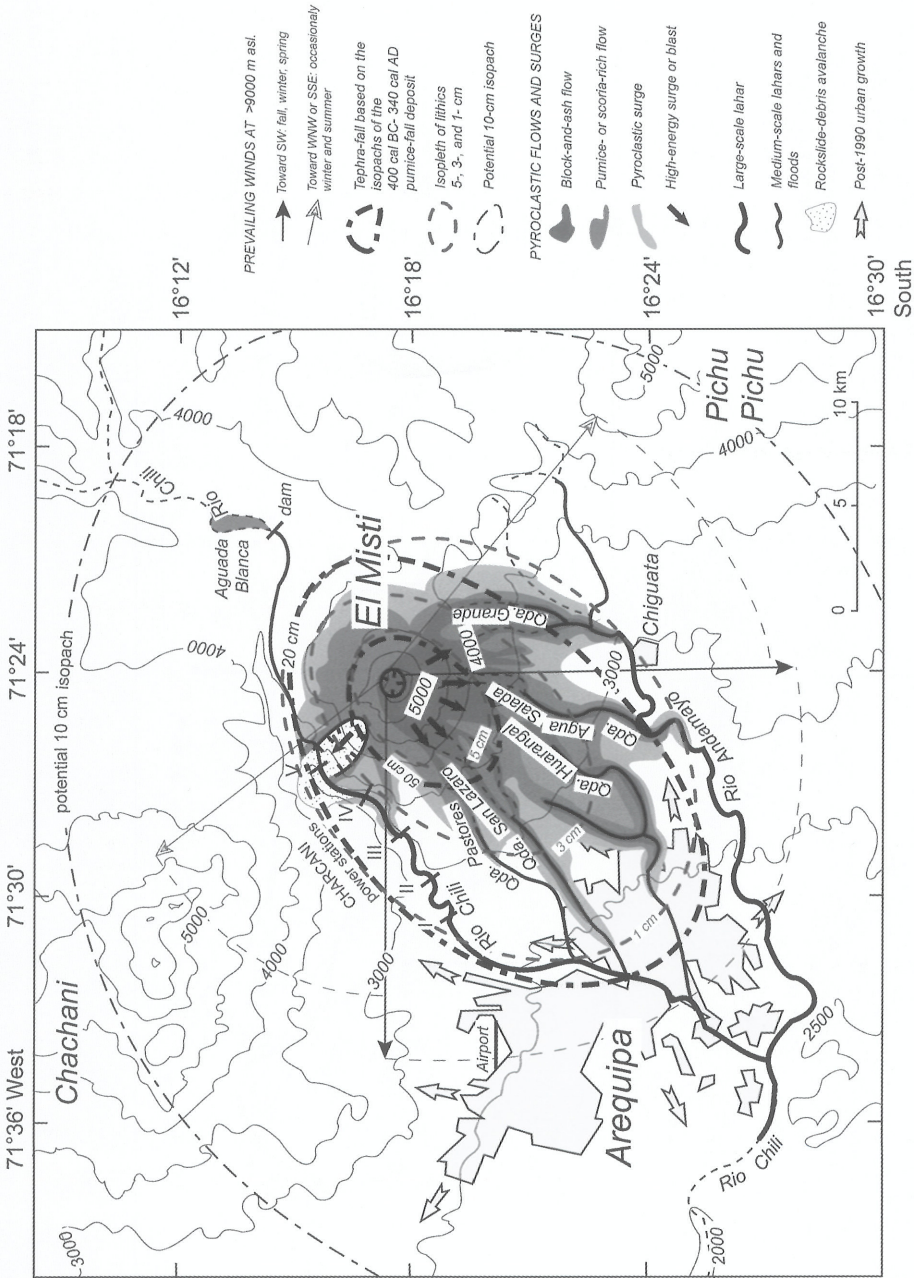based on the AD 1440–1470 vulcanian event.

Fig. 6. Hazard-zone map of El Misti volcano depicting the expected effects of the mid magnitude/mid frequency eruption scenario based on the ca. 2090 yr BP-old sub-Plinian eruptions.
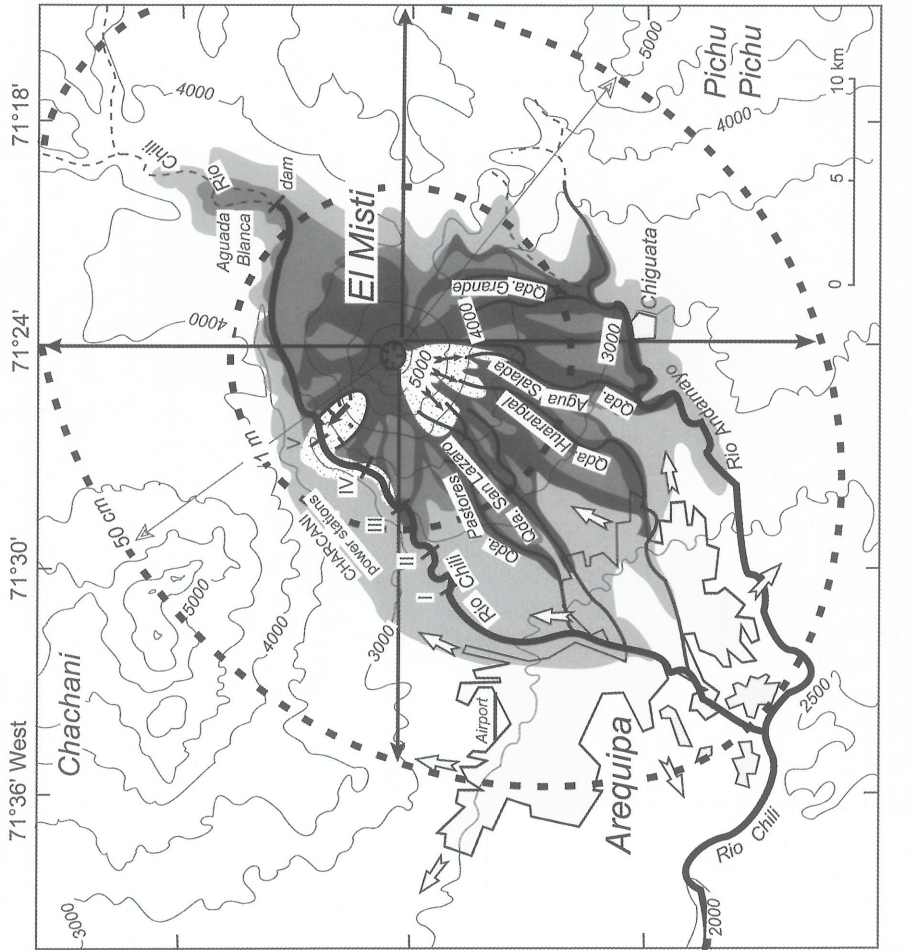
Fig. 7. Hazard-zone map of El Misti volcano portraying the effects of the large magnitude/low frequency eruption scenario based on ca. 34,000–33,000 yr BP and ca. 14,000–11,000 yr BP-old ignimbrite-forming eruptions.

3.3.1 *A low-magnitude* (VEI 2) *and relatively high frequency* (500 to 1500 years) *eruption scenario* is based on the AD 1440–1470 vulcanian events (Fig. 5) and on the 1990–1998 vulcanian and phreatomagmatic activity at Nevado Sabancaya 70 km NW of Arequipa (GERBE & THOURET 2004). Ash falls are expected in Arequipa from eruption columns as low as 3 to 4 km above the vent, as indicated by the isopleths of the 1400's ash-fall deposit. The dispersal of the mid-1400's tephra indicates that ash fall occurred to the N, the W and SW of the cone within 30 km distance. Prevailing winds at 6000–9000 m asl. would carry aloft tephra fall from low columns preferentially toward the NE, should the eruption occur during summer, winter and spring, and toward the west should the event occur at Fall (NCEP/NCAR 1998). The airport 17 km SW of the vent is likely to be affected by ash fall even in the case of a small-scale eruption. As future eruptions will likely disrupt the andesitic plug which taps the younger nested crater, phreatomagmatic events may contribute to destabilising the fractured and hydrothermally altered southern rim of the larger crater. Since a 1 km-wide x 4 km-long scar cuts the unconsolidated rocks of the west summit flank (Figs. 1 and 3), a rockslide-debris avalanche may dam the Río Chili canyon where five power supplies have been built 4–8 km horizontally W and WNW and 2–3 km vertically below the summit. In addition, lahars may be triggered either by snowmelt water or by rainstorms, as suggested by the ca. 330 yr, 520 yr and 1035 yr BP-old lahar deposits that mantle the Río Chili terraces downvalley. Also hyperconcentrated streamflows can occur without eruption, like the 25 February 1997 flash flood along the Qda. Mariano Melgar.

3.3.2 *A moderate magnitude* (VEI 3, volume ≤1 km^3) *and frequency* (2000 to 4000 years) *eruption scenario* may resemble the 2090-yr-old sub-Plinian explosive episode (Fig. 5) and Holocene sub-Plinian events at Ubinas volcano 75 km E of Arequipa (JUVIGNÉ et al. 1997, THOURET et al. 2005). The first hazard is brought about by impact of tephra fall on buildings: the 50-cm and 10-cm isopachs are based on the ca. 2090 yr BP-old pumice-fall deposit found in and around Arequipa. Prevailing winds would disperse ash from eruption columns 5 to 15 km high toward the SW during winter and summer. Occasional winds would carry tephra toward the west during Fall and toward the SE during winter and summer.

The expected direction of future pyroclastic flows is toward the south, owing to the crater wall breached to the S and to the steep south flank. Should a growing dome overtop the crater rim, block-and-ash flows would spill over the summit on the steep slopes of the cone and be channelled as far as 6–10 km from the vent toward the N edge of the town of Chiguata-Arenales and into the NE suburbs of Arequipa. Collapse of sub-Plinian eruption columns can produce pumice flows that would travel longer distances, 10 to 12 km, toward the south, southwest and southeast. Pyroclastic flows at Misti acquire a high momentum due to the H/L ratio (2.4 km height versus 6 km distance between the volcano summit and its foreland), which provides a long runout distance of 11–13 km. The second map also portrays areas potentially swept by pyroclastic surges associated with the pyroclastic flows. Surges may reach the town of Chiguata (about 3500 people) 11 km to the S if a growing dome caused the south crater rim to collapse.

Lahars and stream flows have swept down the radial valleys at least for the past 2000 years, as shown by the 1400's – 1600's and the ca. 1035 and 2090 yr BP-old debris-flow deposits in the Río Chili valley and Quebrada San Lazaro. New suburbs of Arequipa are now spreading upstream

in this area. Large-volume lahars in the Río Chili canyon might result from rockslide debris avalanches if the steep-sided, unstable west flank were to fail above the main power station (Charcani Grande: Fig. 1). Lahars also can be triggered by melt water if pyroclastic debris scoured the summit snowfield from January to August.

3.3.3 The maximum expected pyroclastic eruption (VEI > 4) scenario has a relatively low frequency of 10,000 to 20,000 years based on the ca. 34,000-33,000 and the ca. 13,650–11,280 yr-old ignimbrite-forming eruptive episodes. This scenario includes a 10 to 25 km-high Plinian eruption column whose pumice-fall may produce 1 m and 0.5 m isopachs (Fig. 6); the entire region is likely to be mantled by at least 10 cm of tephra. The prevailing seasonal winds would carry aloft the ash more than 100 km towards the W and SW in winter and spring, and to the NE during summer time. The airport is likely to be severely damaged by a Plinian pumice-fall deposit as thick as 50 cm. A Plinian-type eruption can generate pyroclastic flows spilling over all flanks of the volcano and channeled for at least 15 km in the Río Chili and all tributaries. A light gray area outlines the likely extent of pyroclastic surges that may devastate all the flanks of El Misti and extend to the east flank of Nevado Chachani.

Flank failures could occur on the steep west and south flanks of the volcano. Subsequent debris avalanches would choke the Río Chili valley and devastate the five power supply dams. A debris avalanche from the summit could override the Arequipa basin and continue toward the Batholith, given an H/L ratio of 0.11, i.e. the average value of 40 volcanic debris avalanches worldwide (HAYASHI & SELF 1992). Should H/L equal 0.24, the value for a small-volume debris avalanche, it would reach the city suburbs where hummocks of past avalanches are preserved. Finally, the map also shows valleys that would convey voluminous lahars, in particular the Río Chili canyon. Not only would the five power stations be damaged but also the large Aguada Blanca dam to the north, as well as the cultivated and populated Río Chili valley beyond the city to the south and southwest.

In sum, the first and second hazard-zone maps portray the most likely scenarios for future El Misti's eruptions, although we cannot preclude a worst-case Plinian scenario, such as the 1600 AD Huaynaputina eruption, which deposited as much as 15 cm of ash and lapilli in Arequipa 75 km W of the vent (THOURET et al. 1999b, 2002). However, the most probable event at El Misti would disrupt the present plug and subsequently lead, either to dome growth with block-lava avalanches or block-and ash flows down the steep southern flank, or to a vulcanian regime, which might evolve to a sustained sub-Plinian regime.

4   Simulating lahars with LAHARZ

4.1 First step for simulating lahars with the LAHARZ code

LAHARZ (SCHILLING et al. 1998) is an ArcInfo Macro Language semi-empirical code used for simulating and computing areas 'inundated' by lahars. Simulating lahars encompasses three steps. The first step requires input volumes of measured and dated lahar deposits at El Misti volcano (Table 1). The software achieves a simultaneous calculation based upon four user-speci-

Table 1. Parameters of lahar and alluvium deposits in the radial valleys of El Misti.
([14]C: GrN and LSCE-Gif numbers, conventional dates; GrN, J. van der Plicht, Centre for Isotope Research, Rijksuniversiteit, Groningen, the Netherlands; Lv Louvin, Belgique).

Sample and Lab number	Location (Figs.2, 3, 8)	Material, deposit and terrace	Material dated	[14]C age (yr B.P.)	Calibrated age (1 σ)	Extent and estimated volume
JCT 98-GrN 23885	Yanahuara near church, right bank, 2300 m	Lahar runout on terrace t2a	charcoal	330 ± 60	1400 – 1600 cal A.D.	At least 10 km long, 0.2 km wide, 2 m thick; 4 x 10^{6}m[3]
JCT 98-GrN 23965	Río Chili left bank, Chocita restaurant 2400 m	Streamflow on terrace t3	organic matter in silt	340 ± 40	1488 – 1633 cal A.D.	At least 7 km, 0.1 km wide, 3 m thick; 2.1 x 10^{6}m[3]
JCT 98-GrN 23966	Río Chili right bank, Academia tenis, 2325 m	Upper lahar runout deposit on terrace t2	charcoal	520 ± 25	1407 – 1428 cal A.D.	At least 9 km long, 0.25 km wide, 3 m thick; 6.75 x 10^{6}m[3]
JCT 98-12 Gif-11870	Río Chili left bank, Chilina, 2450 m	Base of lahar runout deposit on terrace t2	charcoal	1035 ± 45	782 – 1018 cal A.D.	At least 6 km long, 0.1 km wide, 2 m thick; 1.2 x 10^{6}m[3]
JCT GrN-23149, 22162, GrA 4398, Lv-2111	Qda. San Lazaro right bank, 2650 m	Pumice-rich lahar deposits derived from pyroclastic-flow deposit	charcoal	2090 ± 85 (=average of four dates)	402 cal BC – 340 cal AD (=largest cal age range)	At least 9 km long, 0.1 km wide, 4 m thick; 3.6 x 10^{6}m[3]
Dating in progress	Rio Chili downvalley, Uchumayo toll, left bank	Lahar (debris-flow) deposit derived from an ignimbrite	Charcoal in pumice-fall deposit beneath	Probably middle Holocene in age	N/A	At least 30 km long, 0.2 km wide, 5 m thick; 30 x 10^{6}m[3]

fied values of volumes, a topographic Digital Elevation Model, and a value of H/L ratio defining an energy cone, H and L being respectively the height of the cone at the knick point and the half diameter at the base of the cone of a given volcano. Computing areas relies on a statistical data base and on two equations (e.g. IVERSON et al. 1998). Equation A for cross section of draining valleys is:

$$A = 0.05 \ V^{2/3},$$

and equation B for planimetric 'inundated' area is:

$$B = 200 \ V^{2/3} \ \text{with} \ V = \text{volume of lahar.}$$

LAHARZ calculates the surface spreading of floods starting from a proximal hazard boundary, defined by the intersection of the energy cone with topography. Nevertheless, the LAHARZ code is not physically based; instead, the semi-empirical simulations allow us to outline the extent of hazard zones prone to lahar flooding based on the magnitude of the events which have occurred in the recent past of a given volcano.

4.2 Second step for simulating lahars with LAHARZ

The calculation parameters are fourfold: (1) a threshold of the maximal height of the irregularities of the DEM to be smoothed; (2) a threshold which defines how streams are selected; (3) a proximal area of non deposition (based on the H/L ratio), and; (4) a choice of lahar volumes based on a field data set. Four operations consist in the: (1) creation of a "smoothed" grid; (2) definition of the proximal hazard zone boundary; (3) choice of the first and last cells of the stream used for simulations, and; (4) simulation of lahars according to four categories of volumes (see scenarios, Fig. 8).
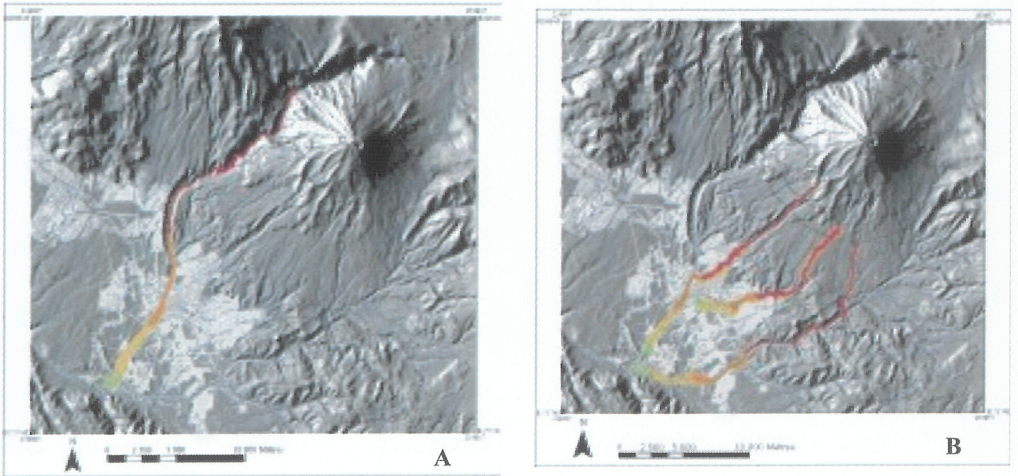

Fig. 8. Simulated lahars that start at El Misti volcano and cross the city of Arequipa. A. Simulated lahars of 0.5, 4, 9, and 11 x 10^6 m^3 in volume in the Río Chili valley. B. Simulated lahars of 0.5, 4, 9, and 11 x 10^6 m^3 in volume in the Quebradas San Lazaro, Huarangal, and Agua Salada.

4.3 Third step for simulating lahars with LAHARZ

The accuracy and sensitivity of the DEM of El Misti volcano have been improved by G. DELAITE (2003) who homogeneized, corrected, and orthorectified digitized data, then merged existing DEMs at the Laboratoire Magmas et Volcans of the Université Blaise Pascal. The accuracy of the El Misti DEM (Fig. 8), originally derived from digitised 1:25,000 topographic maps (>30 m resolution, VAN GORP 2002) and ERS Radar scenes interferometry (30 m resolution, GONZALES 2000), was improved by stereo-photogrammetry technique to pairs of 1:5000-scale aerial ortho-

photos. The resolution has been increased to as much as 8–10 m in the area of the city centre, e.g. the confluence of Río Chili with its left tributary Quebrada San Lazaro. GPS measurements have been carried out in July–August 2003 along profiles across the terrace system (Río Chili) and across two Quebradas, and eventually tied the DEM to three geodetic monuments designed by the U.S. Corps of Engineers in 1964.

4.4 Output maps: lahar-inundated drainage network across Arequipa

The first scenario (Fig. 8A) delineates the valley channel of Río Chili, which can be inundated by four categories of small, medium, and large lahar volumes of 0.5 to 11 x 10^6m^3. The second scenario (Fig. 8B) displays the three tributary channels of *Quebradas* San Lazaro, Huarangal, and Agua Salada, which can be inundated by similar lahar volumes of 0.5 to 11 x 10^6m^3. Relatively small-scale debris flows can recur at least once every one to three centuries or so (see Table 1). Large-scale lahars are much less frequent (once or twice per thousand years) but are not unknown, as indicated by deposits 10 m in height above the present channel, which are interbedded in the middle terraces of the Río Chili valley. However, hyperconcentrated streamflows, which are rainstorm-triggered at present in valleys draining El Misti, are far more frequent than debris flows. Flash floods and hyperconcentrated streamflows can recur as frequently as two to ten years on average (NAGATA 1999), such as the 1992 Río Chili flood and the 1997 hyperconcentrated flow in the Quebrada Huarangal. Flash floods typically remobilize loose pyroclastic and alluvial debris as well as garbage in the channels used as sewage paths across the city. When they are hit by rainstorms >10 mm per hour from December to March, the steep-gradient channels (>15% on the volcano flanks to 5% on the alluvial fans in the city), which cut down coarse-grained deposits, respond rapidly by bulking material and transforming flash floods into hyperconcentrated streamflows.

4.5 Outcomes of computer code simulations

We have carried out LAHARZ tests on four radial valleys which drain El Misti volcano towards Arequipa: the permanent Río Chili and its tributaries Quebradas San Lazaro, Huarangal, and Agua Salada (Fig. 8). The four valleys were selected on the basis of the occurrence of recent (<2000 yr BP) lahar deposits and of the potential danger they pose to the approximately +50,000 city dwellers who live along the valley banks. H/L values were selected from the top of the volcano, at 5822 masl., to the starting point where the lahar deposits were observed in each valley: 0.5 for Río Chili, 0.45 for Qda. San Lazaro, 0.373 for Qda. Huarangal, and 0.332 for Qda. Agua Salada (Fig. 8). The two probable eruptions of El Misti (Figs. 4 and 5; THOURET et al. 2001), which can trigger small- to moderate-sized lahars, form the basis on which the LAHARZ code was tested. The lahar volumes are based on the amount of material which can be mobilized in channels, on rainfall data, and on the seasonal snow field on the volcano summit. Simulations (Figs. 8A and B) show that even a small volume lahar (0.5 to 1.5 million m^3) can reach the suburbs of the city. The large-scale lahars (9 to 11 millions m^3) cross the entire city of Arequipa as far as 30 km downvalley. For example, lahar deposits 5 m thick crop out in the Chili valley as far as 30 km away from the ca. 2050 yr BP-old pyroclastic-flow deposits observed in the Quebrada San Lazaro.

5   Discussion

5.1   Validation of the simulations by back analysis

If we compare the lahars simulations carried out in four draining valleys at El Misti using the LAHARZ code with the actual deposits of the historic and Holocene lahar and hyperconcentrated flow deposits in measured sections across the channels, we observe a fair delineation of the areas affected by potential lahars (Figs. 8 and 9). Fig. 9 shows cross sections in the Río Chili valley (THOURET et al. 1999) from the entrance of the canyon 8 km north of the center of Arequipa downvalley to 2 km south of the city centre. Terraces, which have been measured in field surveys and located on 1:5000 scale orthophotos, are covered by lahar and streamflow deposits. From the oldest to the youngest, three pairs of terraces are as follows (Figs. 9A, B and C):

— Terraces t1 and 1a, approximately 20 to 25 m above the channel, have not been dated. Terrace t1 is younger than ca. 40,000 yr BP, the age of pyroclastic-flow deposits upstream in the Río Chili valley. Lahar deposits observed as far downvalley as 30 km from el Misti knickpoint may have a volume in the range of 10 to 30 million m^3.

— Terraces t2 and 2a, about 10–15 m above the present channel, are composed of pyroclastic-flow, lahar and hyperconcentrated streamflow deposits, and alluvium. Holocene in age, they have been covered by ^{14}C dated lahar deposits at ca. 1035 and 520 yr BP. Historical lahar deposits of ca. 320 yr B.P., which may be attributed to the mid 1400's events, mantle the terrace t2 at 9.5 m above the present channel in the Yanahuara district < 2 km N of the city centre. The volume of the 3 m-thick lahar deposits is estimated to be in the range of 4 to 6.75 million m^3.

— Terrace t3, 3–4 m above the channel, is probably of Pre-Colombian historical age. A lahar runout deposit which mantles that terrace has been dated at ca. 340 yr B.P. (Table 1). The volume of the 2 m-thick lahar deposit ranges between 1.2 and 2.1 million m^3.

— Terrace t3a, 2-3 m above the channel, consists in two or three steps cut in the t3 terrace, which are younger than 300 years. The t3a terrace is easily inundated in case of a 10-yr interval flood.

Historical deposits younger than the Spanish Conquest in AD 1540 point to the extent of Río Chili floods and of potential lahars of approximately 0.5 to 2 million m^3, which can spread toward the lower part of the city center. A trimline of gravel, sand, and mud is plastered as high as 10 m above the channel against the NW wall of the narrow Río Chili canyon at the Charcani sanctuary (Fig. 9A). In February 1992, a flood (Q = 260 m^3/sec) in the Río Chili valley overran the new bridge below the Colonial Puente Grau bridge (Fig. 9C) and damaged the city dwellings and the main road on the left bank terrace t3a. These deposits and the trimline witness to modern floods which may recur on a 10 to 20 year interval.
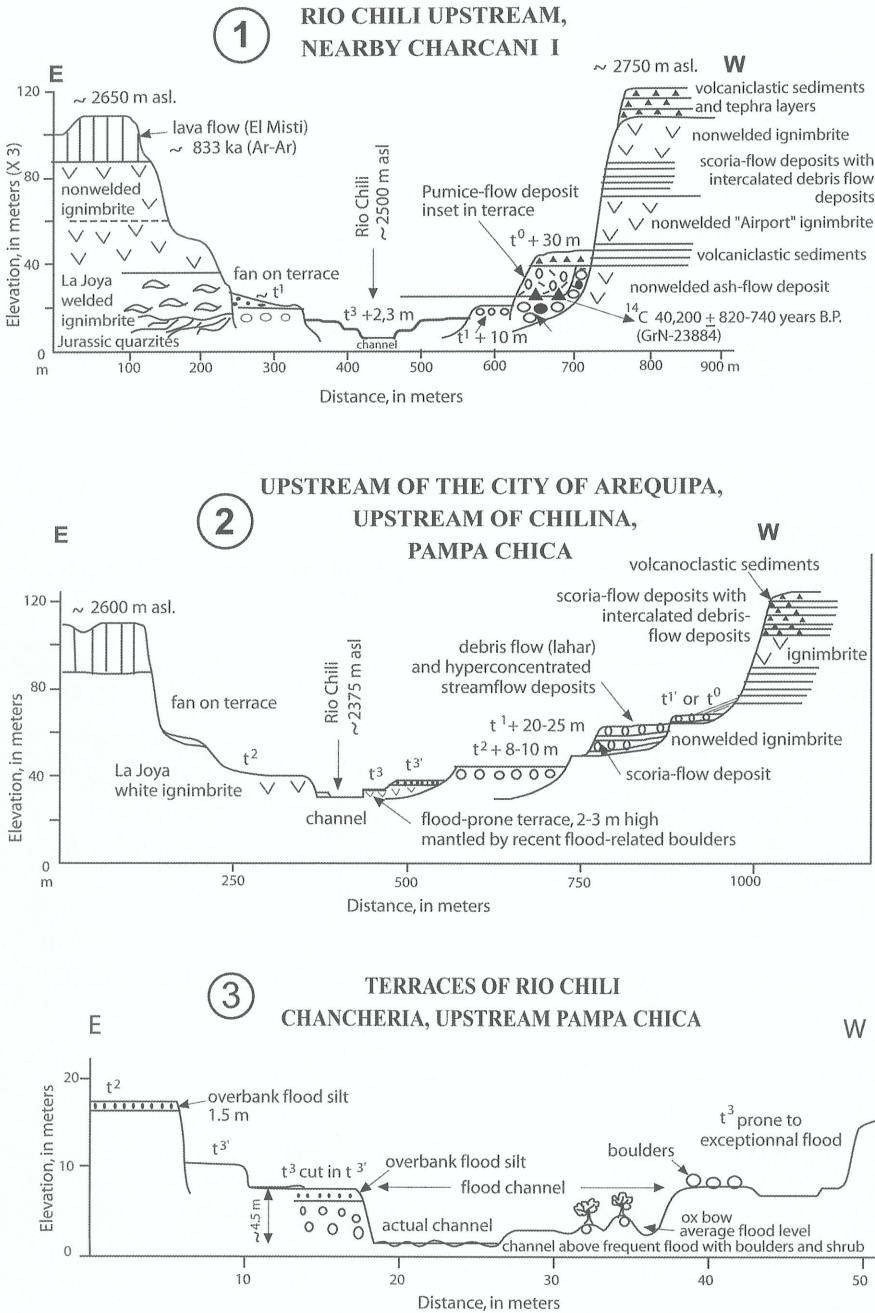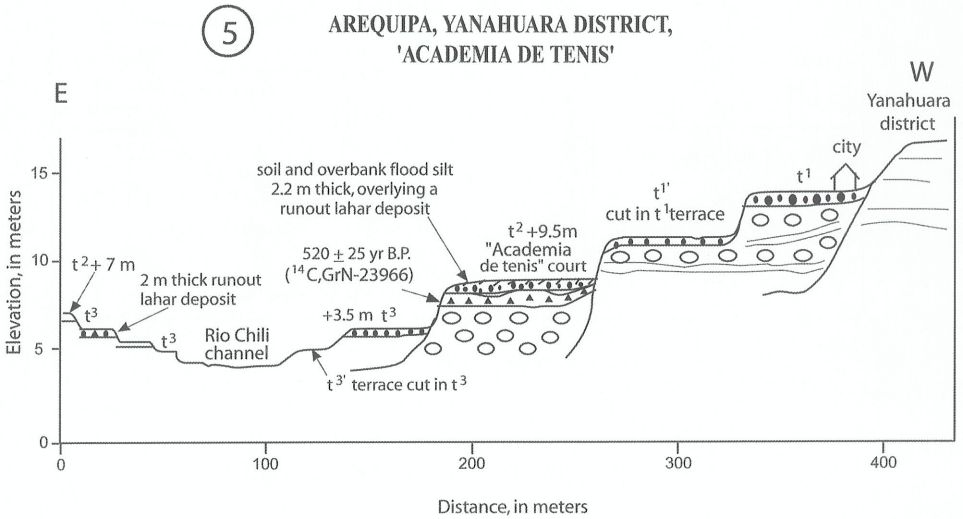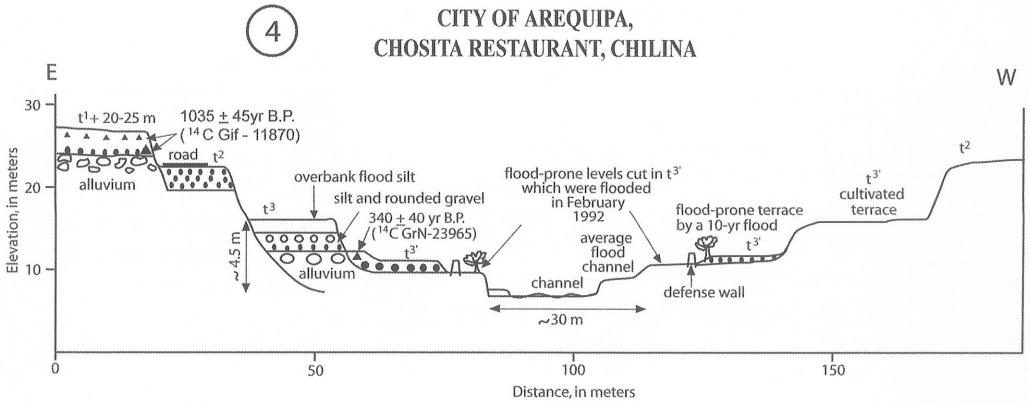
Fig. 9. For the purpose of validating the simulated lahars, seven cross sections show measured and dated lahar deposits on the Río Chili valley terraces upstream and in the city centre of Arequipa: 9A − 1. Río Chili upstream, nearby Charcani I; 9A − 2. Río Chili upstream, upstream of Chilina, Pampa Chica − 3. Chancheria, upstream of Pampa Chica.

Fig. 9. For the purpose of validating the simulated lahars, seven cross sections show measured and dated lahar deposits on the Río Chili valley terraces upstream and in the city centre of Arequipa: 9B – 4. City of Arequipa, Chosita Restaurant, Chilina 2 km upstream of cross section 5; – 5. Arequipa, Yanahuara district, Academia de Tenis.

5.2 *Needs and drawbacks to the code*

On the one hand, according to the tests carried out in the frame of this study and at similar volcanoes (Pareschi et al. 2000 at Vesuvius; Stevens et al. 2003 at Ruapehu), LAHARZ yields plausible results provided it runs on an accurate topographic Digital Elevation Model and uses
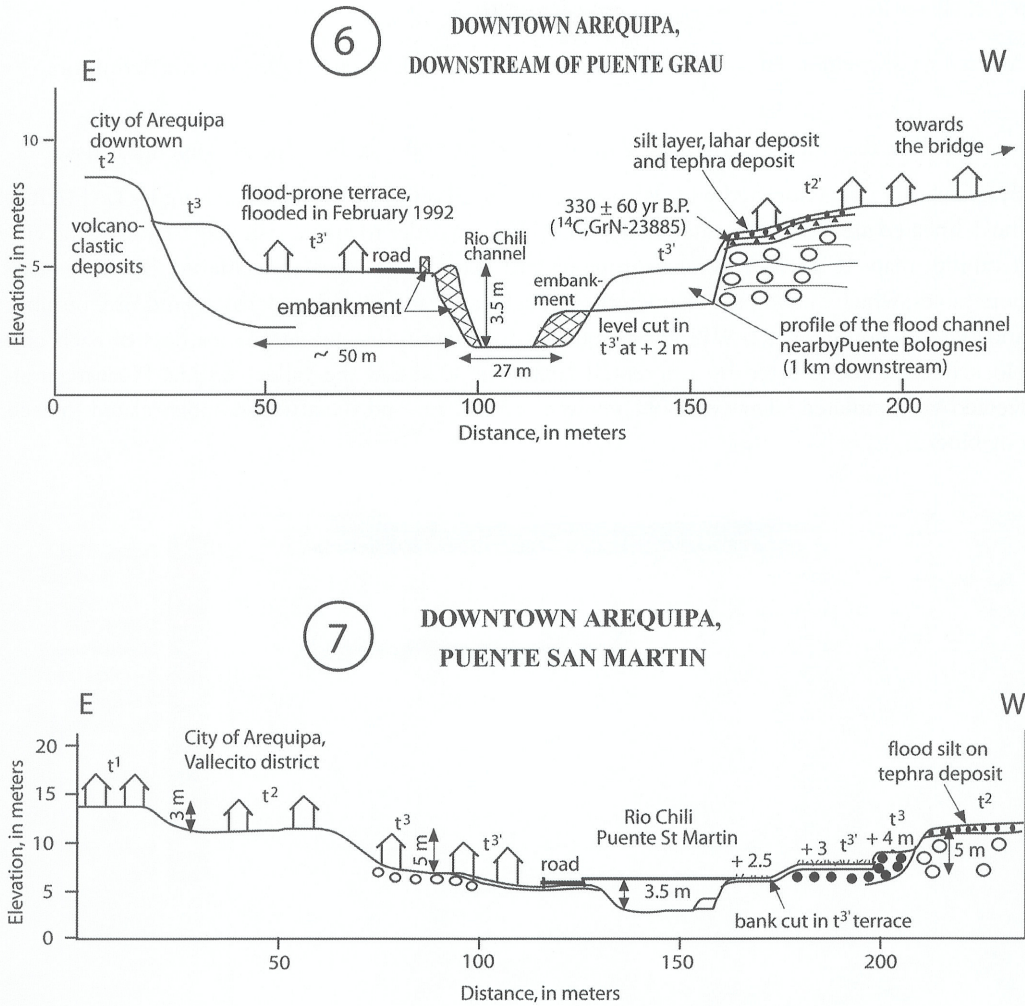
Fig. 9. For the purpose of validating the simulated lahars, seven cross sections show measured and dated lahar deposits on the Río Chili valley terraces upstream and in the city centre of Arequipa: 9C – 6. Downtown Arequipa, downstream of Puente Grau; 9D – 7. Downtown Arequipa, Puente San Martin.

realistic, field-based values of lahar volumes. On the other hand, a few drawbacks of the code have also been highlighted, such as the disability to run the code in two streams at the same time or on convex fans. In addition, LAHARZ, a semi-empirical code, does not account for physical parameters of lahars, which are critical. For example, the bulking factor, i.e. the material incorporated to the flows in the channel, is not accounted for. This bulking factor is likely to play a major role in the gullies which drain the flanks of the volcano upstream of the intersection of H with L.

6   *Risk assessment*

Assessing risks requires a combination of vulnerability with hazard, following the definition:

$$R = H * V * Va,$$

with R as the risk, H the hazard, V the vulnerability, and Va the value of elements at risk.

By evaluating risk associated with lahar hazards, based on simulations carried out by LAHARZ, the delineated areas are integrated in the GIS ILWIS in order to create risk maps. By crossing vulnerability maps (Fig. 10) with lahar-prone hazard maps, risks maps are achieved. By using attribute tables, which encompass characteristics such as area, population density, land use, number and type of house, etc., ILWIS allows queries for identifying vulnerable features of each city block likely to be affected by a potential lahar. Fig. 10 shows the valley of Qda. Huarangal affected by a simulated lahar event of a volume of 11.10^6 m^3 and the attribute table related to each city block.
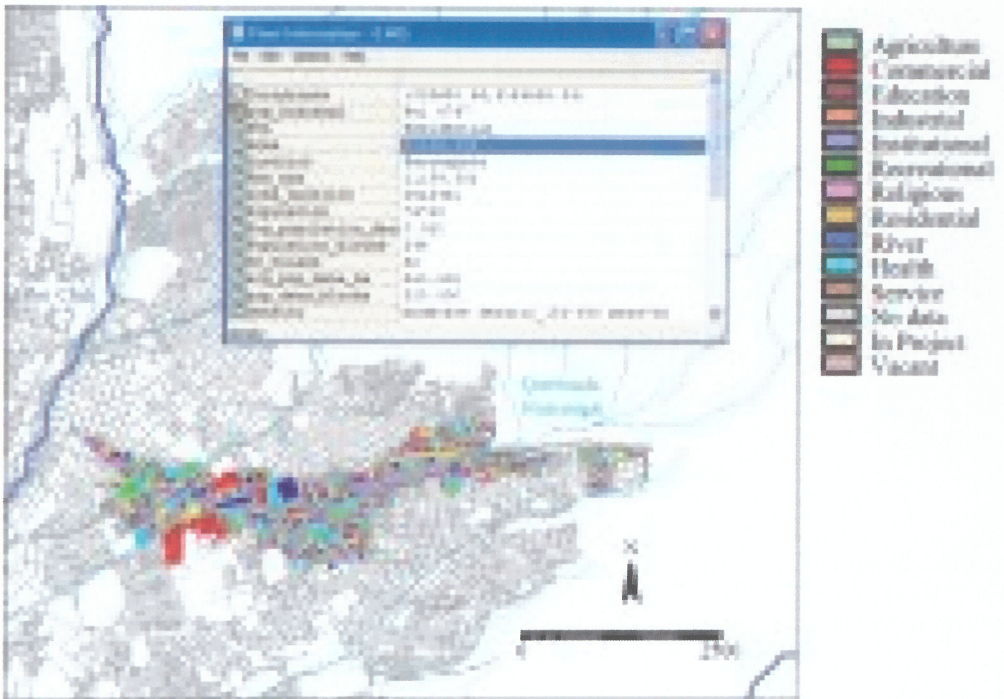

Fig. 10. Risk map in the GIS ILWIS, which combines hazard zone with vulnerable elements at stake. An information layer on land use in the city district of Huarangal-Mariano Melgar overlays the area of the Quebrada Huarangal affected by a simulated large-scale (11×10^6 m^3) lahar. Information on social and economical parameters of each city block can be obtained through queries using attribute tables (inset).

7   Conclusions

7.1 Summary

Hazards at El Misti have been identified: ashfall, pumice fall, block-and ash flow, scoria fall and flow, pumice and ash flow, debris avalanche, and lahar. The most probable eruption scenario will consist of a phreatomagmatic disruption of the present plug, a vulcanian ash fall, and maybe block-and-ash flows, should a dome grow above the crater. The areas likely to be affected are firstly the south flank, the west flank, and the radial drainage that convey lahars and pyroclastic flows toward the city of Arequipa, in particular the Río Chili canyon where a large dam and five power supplies are at risk. The simulations of areas likely to be inundated by four categories of lahar scenarios show that lahars, even medium sized (1 to 2 x 10^6m^3), will cross the city of Arequipa.

7.2 Perspectives

Results from the research bear on prevention measures to be applied in the city area of Arequipa. The simulation and modelling embedded in a GIS can be user friendly, updated during a crisis, and used almost in real time. New risk maps, based on scenarios and simulations and crossed with vulnerability maps, provide readily and timely available information through queries. The risk evaluation will include a survey and cost effective analysis of potential damages on buildings near the lahar-prone channels. Risk maps may serve as a tool for the process of emergency measures and decision making by the Civil Defense in Arequipa and by civil authorities.

To validate the simulations using the LAHARZ code, there is a need to: (1) improve the DEM accuracy, (2) enhance the quality of the data base, and (3) add geotechnical characteristics of deposits, which help to estimate the amount of material to be remobilised in channels and the rate of bulking process. We need to improve the DEM accuracy and resolution, and the computation of real lahar volumes in order to better simulate lahars while taking account of the lahar behaviour in channels and on alluvial fans. More recently, TITAN2D simulations have been carried out using the DEM of El Misti (STINTON et al. 2004). Work in progress shows that the simulated lahars using TITAN2D provide a better approach since the computer code is based on a model of shallow-water geophysical flows, which includes friction coefficient at bed and reproduces more faithfully the behaviour of the lahars (THOURET et al. 2005).

Finally, our risk maps may contribute to the management of future volcanic crises. People at risk are those who live in the channels of the studied Río Chili and Quebradas San Lazaro and Huarangal. Infrastructures likely to be damaged are those which have been constructed in the path of potential debris avalanches and lahars in the Río Chili valleys. Evacuation routes should be enlarged and properly paved toward the town of Yura 30 km to the west and, more safely, to the SE (Yarabamba and Chapi), if a bridge is to be built on the Río Tambo valley.

References

Barriga, V.M. (1951): Los terremotos en Arequipa (1582 – 1868). – 426 pp.; La Colmena, Arequipa.

Blong, R. (1984): Volcanic hazards: a sourcebook on the effects of eruptions. – 424 pp., Academic Press, San Diego.

Blong, R. (2000): Assessment of Volcanic Risks. – In: Sigurdsson, H. et al. (eds.): Encyclopedia of Volcanoes. – pp. 1215–1225; Academic Press; San Diego.

Chávez Chávez, J.A. (1992): La erupción del volcán Misti. Pasado, presente, futuro. – 158 pp., Impresiones Zenit, Arequipa.

Chester, D.K., Degg, M.R., Duncan, A.M. & Guest, J.E. (2001): The increasing exposure of cities to the effects of volcanic eruptions: a global survey. – Environm. Hazards **2**: 89–103.

Delaite, G. (2003): Méthodes pour le diagnostic des risques volcaniques fondées sur les Systèmes d'Information Géographique et le code de simulation LAHARZ. – 55 pp., DEA Processus magmatiques et métamorphiques; Volcanologie, Université Blaise-Pascal, Clermont-Ferrand.

Gerbe, M.-C. & Thouret, J.-C. (2004): Role of magma mixing in the petrogenesis of lavas erupted through the 1990-98 explosive activity of Nevado Sabancaya in south Peru. – Bull. Volcanol. **66**: 541–561.

Gonzales, K. (2002): Mise au point d'une méthode d'amélioration de Modèles Numériques de Terrain à partir d'interférogrammes radar. Application à la région d'Arequipa, Perou. – 50 pp., Mémoire de DUPV; Université Blaise Pascal, Clermont-Ferrand.

Hantke, G. & Parodi, I.A. (1966): Catalogue of the Active Volcanoes of the World. Part XIX: Colombia, Ecuador and Peru. – 73 pp.; IAVCEI, Naples.

INEI-ORSTOM (1998): El Perú en Mapas. Atlas en base al censo de población y vivienda. – 140 pp.; Institut de Recherche pour le Développement, Lima.

Iverson, R.M., Schilling, S.P. & Vallance, J.W. (1998): Objective delineation of lahar-inundation hazard zones. – Geol. Soc. Amer. Bull. 110 (8): 972–984.

Juvigné, E., Thouret, J.-C., Gilot, E., Gourgaud, A., Legros, F., Uribe, M. & Graf, K. (1997): Etude téphrostratigraphique et bioclimatique du Tardiglaciaire et de l'Holocène de la Laguna Salinas, Pérou méridional. – Géogr. physique Quatern. **51** (2): 219–231.

Macedo, L.F. (1994): Peligro volcánico potencial del Misti. – Tesis de grado (unpubl.), 112 pp.; Universidad Nacional San Agustín, Convenio DHA-UNDRO-UNSA, Arequipa.

Nagata, M. (1998): Una introducción a las inundaciones en el area urbana de Arequipa. Informe sobre las torrenteras en Arequipa. – 99 pp.; INDECI-IGP-ORSTOM, Lima.

Navarro, P. (1998): Geología del volcán El Misti. – Tesis de grado, 125 pp. (unpubl.); Instituo Geofísico del Perú, Lima y Universidad Nacional San Agustín, Arequipa.

NCEP/NCAR (1998): National Center for Environmental Prediction-National Center for Atmospheric Research, Climate Data Assimilation system, Reanalysis Project, monthly mean data from the period 1979–1995. Web site: http://www.gfdl.gov/ ~ jjp/ncap_data.html

Pareschi, M.T., Cavarra, L., Favalli, M., Giannini, F. & Meriggi, A. (2000): GIS and volcanic risk management. – Natural Hazards **21**: 361–379.

SCHILLING, S.P. (1998): LAHARZ: GIS program for automated mapping of lahar-inundation hazard zones. – U.S. Geol. Surv. Open-File Rep. **98-638**.

SIMKIN, T. & SIEBERT, L. (1994): Volcanoes of the World. – 2nd ed., 349 pp.; Smithsonian Institution, Geosciences Press Inc.

STEVENS, N.F., MANVILLE, V. & HERON, D.W. (2002). The sensitivity of a volcanic flow model to digital elevation model accuracy: experiments with digitised map contours and interferometric SAR at Ruapehu and Taranaki volcanoes, New Zealand. – Journ. Volcanol. Geotherm. Res. **119**: 89–105.

STINTON, A., DELAITE, G., BURKETT, B., SHERIDAN, M., THOURET, J.-C. & PATRA, A. (2004): Titan2D simulated debris flow hazards: Arequipa, Peru. – Abstract, ISESS, International Symposium on Environmental Software Systems, USA, March 2004.

SUNI, J. (1999): Estudio geológico y vulcanológico del volcán Misti y sus alrededores. – 179 pp., Tesis de posgrado (unpubl.); Instituto Geofísco del Perú, Lima and Universidad Nacional San Agustin, Arequipa.

THOURET, J.-C., LEGROS, F., GOURGAUD, A., SALAS, G., JUVIGNE, E., GILOT, E., URIBE, M. & RODRIGUEZ, A. (1995): Un exemple de prévision des risques volcaniques au Pérou méridional (région d'Arequipa), fondé sur l'étude de l'activité éruptive récente du strato-volcan El Misti. – C.-R. Acad. Scis. Paris, t. **320** (sér. IIa): 923–929.

THOURET, J.-C., SUNI, J., EISSEN, J.PH. & NAVARRO, P. (1999a): Assessment of volcanic hazards in the Arequipa area based on the eruption history of Misti volcano, southern Peru. – Z. Geomorph. N.F., Suppl.-Bd. **114**: 89–112.

THOURET, J.-C., DÁVILA, J. & EISSEN, J.PH. (1999b): Largest historic explosive eruption in the Andes at Huaynaputina volcano, southern Peru. – Geology **27** (5): 435–438.

THOURET, J.-C., FINIZOLA, A., FORNARI, M., SUNI, J., LEGELEY-PADOVANI, A. & FRECHEN, M. (2001): Geology of El Misti volcano nearby the city of Arequipa, Peru. – Geol. Soc. Amer. Bull. **113** (12): 1593–1610.

THOURET, J.-C., DÁVILA, J., JUVIGNE, E., GOURGAUD, A. & BOIVIN, P. (2002): Reconstruction of the AD 1600 explosive eruption at Huaynaputina volcano, Peru, based on geologic evidence and Spanish chronicles. – J. Volcanol. Geotherm. Res. **115** (3-4): 529–570.

THOURET, J.-C., SHERIDAN, M., STINTON, A., LABAZUY, PH. & SOURIOT, T. (2004): Hazard and Risk Assessment around el Misti volcano and in the city of Arequipa, Peru, based on GIS and simulation codes. – IAVCEI General Assembly (14–19 November 2004); Pucón, Chile; publ. Abstract, session 5.

THOURET, J.-C., RIVERA, M., WÖRNER, G., GERBE, M.-C., FINIZOLA, A., FORNARI, M., GONZALES, K. (2005): Ubinas: evolution of the historically most active volcano in Southern Peru. – Bull. Volcanol. **67** (in press, online 25 May 2005, Springer link).

VAN GORP, S. (2002): Systèmes d'Information Géographique et risques volcaniques: approche méthodologique et application au cas du volcan Misti et de la zone urbanisée d'Arequipa, sud du Pérou. – 25 pp., Bachelor thesis (unpubl.), Laboratoire Magmas et Volcans, Université Blaise-Pascal, Clermont-Ferrand.

ZAMACOLA, Y. & JAUREGUI, J.D. (1804): Apuntes para la historia de Arequipa. – 15 pp.; Primer festival del libro arequipeño, Edición 1958, Arequipa.

Addresses of the authors: G. Delaite, J.-C. Thouret, Ph. Labazuy and Th. Souriot, Département de Géologie, Laboratoire Magmas et Volcans, Université Blaise Pascal, 5 rue Kessler, 63038 Clermont-Ferrand cedex, France (thouret @opgc.univ-bpclermont.fr; Phone : +33 4 73 34 67 44 ; Fax: +33 4 73 34 67 44).
C. van Westen, ITC International Institute for Geo-Information and Earth Science, Enschede, The Netherlands.
M. Sheridan and A. Stinton, Department of Geology, University of Buffalo, Buffalo, NY, USA.